The 8th International Supercritical CO_2 Power Cycles Symposium
February 27 – 29, 2024, San Antonio, Texas
Paper #73

Experimental Demonstration of a Coal Fired Primary Heat Exchanger in a sCO_2-based Power Cycle

Kyle P. Sedlacko
Sr. Mechanical Systems Engineer
Echogen Power Systems (DE), Inc
Akron, Ohio

Jason Miller
Director of Engineering
Echogen Power Systems (DE), Inc
Akron, Ohio

Brett Bowan
E,I and C Manager
Echogen Power Systems (DE), Inc
Akron, Ohio

Dr. Timothy Held
Chief Technology Officer
Echogen Power Systems (DE), Inc
Akron, Ohio

Dr. Andrew Fry
Associate Professor, Chemical Engineering
Brigham Young University
Provo, Utah

Brian Schooff
PhD Candidate
Brigham Young University
Provo, Utah

Rajarshi Roy
PhD Candidate
Brigham Young University
Provo, Utah

Michael D Johnson
Sr. Engineer
Babcock Power
Marlborough, Massachusetts

Andrew P. Chiodo
Program Manager
Reaction Engineering International
Midvale, Utah

Abstract

Heat transfer is fundamental to every thermodynamic cycle, and heat exchangers serve as the mechanism through which energy within a system interacts with a process. These crucial components establish the link between fundamental thermodynamic principles and performance of thermodynamic cycles. The pursuit of increased efficiency of system components, aimed at enhancing overall cycle performance, stands as a primary goal for designers, operators, and owners alike. Higher temperature and pressure applications are becoming more common in many industries and particularly, with sCO_2 based combined cycle applications. These high energy conditions present unique challenges that even the most experienced heat exchanger manufacturers struggle with.

As the implementation of sCO_2 based power systems increases, the benefits accompanying the use of this energy dense fluid continue to prove advantageous techno economically. Indirect sCO_2 power systems have the potential to unlock transformational improvements in efficiency, cost, footprint, and water utilization. A concept study performed as part of the Department of Energy's Coal FIRST (Flexible, Innovative, Resilient, Small, Transformative) Initiative identified the coal-fired primary heater as a critical component requiring further development to enable its subsequent design, fabrication, delivery, and operation.

The focus of this paper is to examine the experimental data acquired through pilot-scale testing of a primary heat exchanger, both from a component and system perspective, operating under utility scale coal-fired boiler conditions. During this discussion, we will review modeling techniques used for optimizing both the fireside and tube-side behaviors of the primary heater. Additionally, we will explore the design, construction, and integration of the pilot-scale primary heater into the furnace. Lastly, we will examine the sCO_2 equipment set including key features and instrumentation needed to evaluate the relationship between sCO_2 flow distribution and heat flux at various firing rates and load transitions.

Introduction

Most of the power generation in the world comes from the application of two thermodynamic cycles – the Rankine cycle and the Brayton cycle. Coal-fired utility boilers and nuclear power plants use the steam-Rankine cycle to heat and pressurize steam which then drives the steam turbines to generate electricity. This is a closed-loop process where the water/steam is indirectly heated through the water walls of the boiler. In natural gas-fired power plants, the natural gas is combusted which increases the temperature and pressure of the combustion products (flue gases) which in turn drives the gas turbines to generate electricity. This is an open-loop process where the flue gases are then released into the atmosphere. In general, the Brayton cycle gas has higher efficiency than the Rankine cycle due to its higher operating temperatures. In recent years, efforts have been made to take the best out of these two cycles to create a supercritical carbon dioxide (sCO_2) Brayton cycle which has higher efficiency and can be operated in a closed loop. The current state-of-the-art of sCO_2 cycles for power generation can be found in the literature [1, 2].

Currently, efforts have been made to increase the efficiency of utility boilers and decrease the emissions from power plants. Several government agencies and private industries are funding projects to enable the energy industry towards a path of cleaner production. sCO_2-Brayton cycle has the potential to increase energy efficiency (which in turn decreases the emissions per MW of power generation) and reduce water consumption. Also, carbon dioxide is one of the primary components of combustion flue gas. If the boilers are retrofitted with carbon-capture technology, they can act as the sole source of the working fluid in a sCO_2-Brayton cycle. Additionally, carbon capture can decrease carbon dioxide emissions making the process close to carbon neutral.

Carbon dioxide is a non-combustible, non-toxic, and inexpensive fluid. Using supercritical carbon dioxide as a working fluid in power production applications has certain advantages over steam. sCO_2 has the density of a liquid and the fluidity of a gas. This characteristic can be useful in lowering capital and operating costs in power plants since the turbomachinery required to use sCO_2 is much smaller than steam turbines [3]. Most of the water walls in steam-Rankine cycles are isothermal walls since a major part of the heat is utilized to vaporize the liquid water by increasing the latent heat. sCO_2-Brayton cycle does not change phase in the loop. sCO_2 is in a supercritical phase throughout the four main processes of the thermodynamic cycle (pumping/compression of the fluid, heat input to the fluid, pressure decrease of the fluid to drive the turbines, and heat rejection from the fluid). Steam on the other hand continuously changes phase from liquid to gas in a Rankine cycle. Also, since the phase does not change for sCO_2, it can be used as a heat sink in a wide range of applications like nuclear [4], coal [5], geothermal [6], concentrated solar power [7], etc. for waste heat recovery from a range of temperatures [8, 9].

In the current work, the performance of a pilot-scale power plant retrofitted with the sCO_2-Brayton cycle has been studied in detail. It was primarily a US Department of Energy funded project to explore what the power plants of the future might look like. The project collaborators include Brigham Young University (BYU), Echogen Power Systems, Reaction Engineering International (REI), Riley Power Inc. (RPI), Linde, and the San Rafael Energy Research Center (SRERC). The tests were conducted in a pilot-scale combustor (which acted as the heat input of the sCO_2-Brayton cycle) located at the SRERC, in Orangeville, Utah. Computational fluid dynamics (CFD) models were run by REI, to understand the thermal energy release and the flow dynamics which formed the basis of the construction of the retrofitted combustor. REI designed and fabricated the heat exchanger which was placed inside the combustor. Echogen designed, built, and delivered the sCO_2 circulation system which integrates the remaining process equipment for the sCO_2-Brayton cycle (pump, turbine, and heat rejection). It should be noted that because turbomachinery construction at these temperatures is extremely costly and technically

challenging, a throttling valve was used instead as it provided the flexibility to change conditions and study the different parameters. Linde provided the carbon dioxide used in the tests. BYU was responsible for managing the project and building the reactor to its current configuration.

Results and Discussion

Materials and Methods

The L1500 Combustor

A 1500 kW_{th} pilot-scale entrained flow combustor (L1500), located at the San Rafel Energy Research Center (SRERC) in Orangeville, Utah, USA, was used in this project. This is a refractory lined furnace with flame temperature, time-temperature profile, turbulent mixing conditions, and particle residence time which are similar to that of a full-scale suspension-fired utility boiler. The combustor is equipped with a dual register low-NOx swirl burner with register velocities and turbulence scales representative of utility-scale burners. The burner has different entry points for the primary air, inner secondary air, and outer secondary air. The combustor has a radiant, a transition, and a convective section. The convective section contains a water-cooled cross-flow heat exchanger which is intended to reduce the flue gas temperature before it enters the baghouse. The radiative section is 14.6 m in length and has a 1 m^2 cross-sectional flow area and is divided into twelve sub-sections.

The fuel is transported from a gravimetric feeder by the primary air to the burner. A gas sample probe is present in the transition section, which is situated between the radiative and the convective sections. Additionally, the combustor has a secondary air input system, a baghouse, and a cooling tower circulation system. Figure 1 shows the general arrangement model of the furnace while Figure 2 - Figure 4 are images of the respective components. This furnace has been utilized in many government and industrially funded projects investigating fuel switching and emission characterization [10-14].

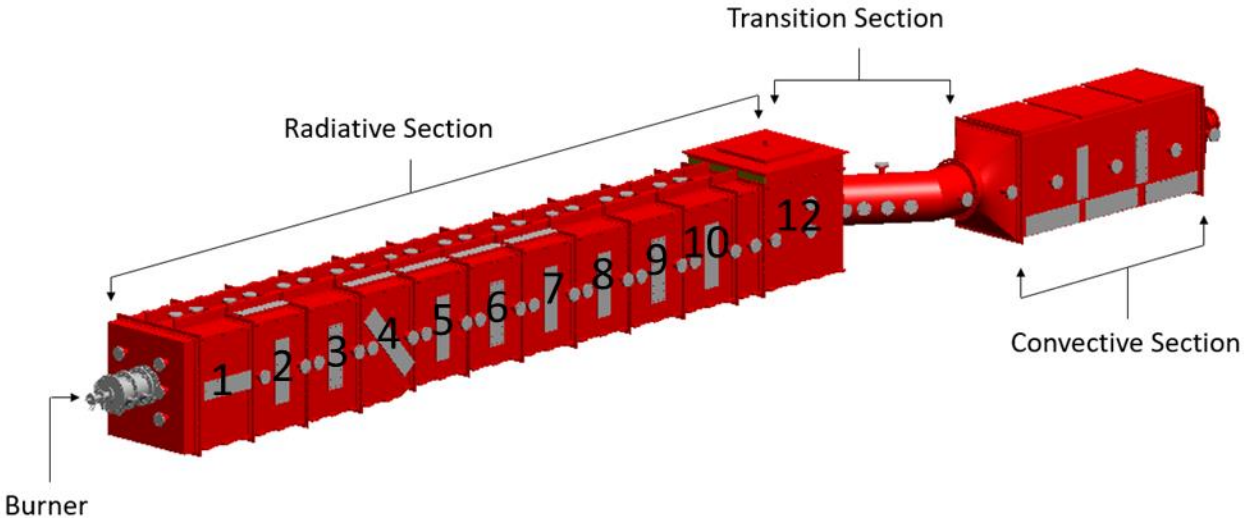

Figure 1. Schematic of the L1500. Adapted from [14].

Figure 2: L1500 Burner Section

Figure 3: L1500 Radiant Section (Foreground) with Transition and Convective Sections (Background)

Figure 4: L1500 Transition and Convective Sections

The radiant section of the L1500 was retrofitted with a primary heat exchanger (PHX), which is comprised of several heat exchange tubes, to test the performance of supercritical carbon dioxide (sCO_2) as the working fluid. Figure 5 shows the schematic of the retrofitted combustor. The light blue tubes represent the portion of the PHX the primarily receives radiant heat (radiant module) and the purple tubes represent the portion that primarily receives convective heat (convective section).

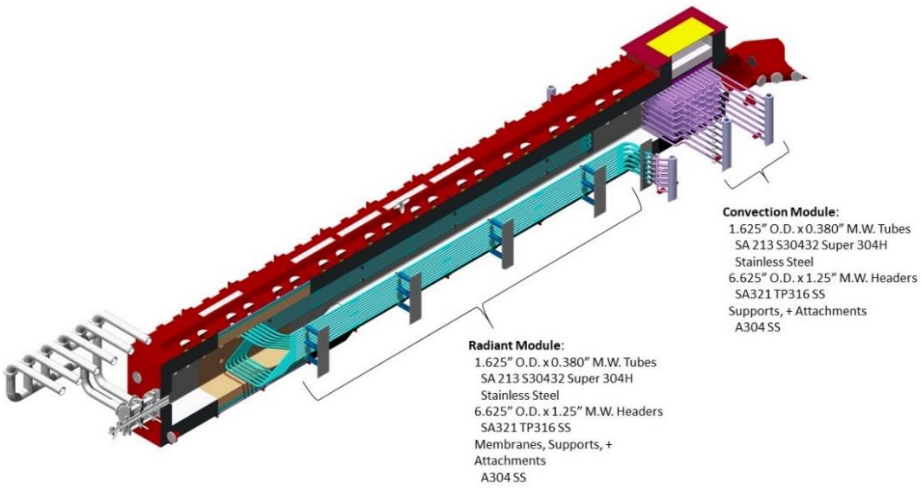

Figure 5. Initial design conceptual of the sCO2 primary heat exchanger with Radiant and Convective Modules in the L1500 furnace.

sCO_2 Thermal Management System

Echogen was tasked with delivering a packaged sCO_2 system (Thermal Management System) capable of achieving the target test conditions for the primary heat exchanger. The conditions for this test are representative of the Brayton recompression power cycle as are highlighted in the P-h diagram shown in Figure 6.

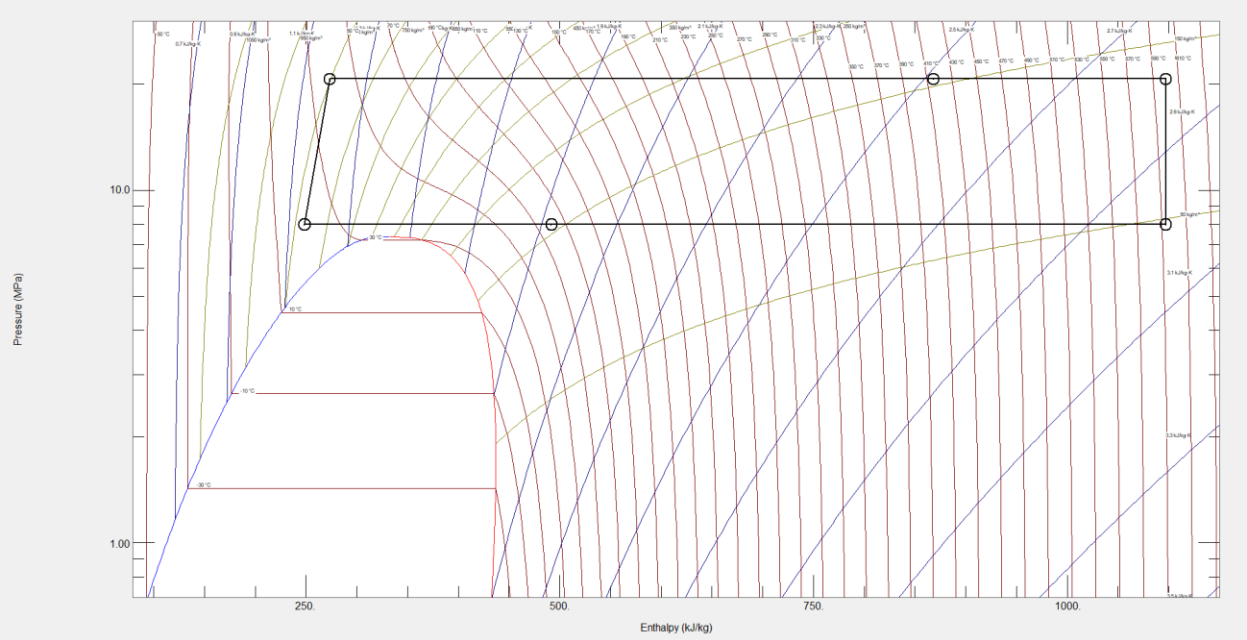

Figure 6: Idealized Process P-h diagram for sCO_2 Cycle

The equipment set selected for this application includes a pump, a recuperative heat exchanger, an expansion valve to simulate the effects of a turbine, a condenser, an active inventory system, and integrated instrumentation and controls.

A thorough examination of the hardware requirements was carried out, pinpointing crucial stages in the process that required further attention to align with the design specifications for the L1500 test. Those areas included pipe material selection, expansion valve selection, pipe stresses and nozzle loads, and safety systems.

While most of the pipe specifications used in the Thermal Management System were considered standard, the PHX return piping was an area which required additional consideration due to the combination of elevated temperature and pressure at the target operating conditions. As a result, SA312-TP316H, a high carbon variant of 316 stainless steel, was selected for these piping components. The alloy's inherent corrosion resistance, particularly in aggressive environments, ensures durability of the piping system. SA312-TP316H is known for its high-temperature strength and creep resistance, providing reliability and structural integrity under extreme conditions. Additionally, the material exhibits excellent mechanical properties, contributing to the overall safety and performance of the piping system.

The expansion valve, otherwise known as a throttle valve, was critical to the operation of the Thermal Management System. In this application, the expansion valve is representative of a turbine, as it induces an irreversible pressure drop. In this case, the losses are in the form of heat due to friction and other dissipative effects. Because of the extreme operating conditions of this system, many of the valve components required enhancement to achieve performance and operability requirements. Some of the features which were considered include, material selection, trim design and selection, actuator sizing and noise attenuation.

PHX Design

The design of the primary heat exchanger (PHX) was intended to cover a number of testing and analysis goals, while following best practices for surface layout and fabricability. The major constraints on the system are operating and design temperatures and pressures. Flow rates, heat flux, pressure drops, and other design factors are also considered during the layout of the system and the selection of materials.

The PHX for this project was designed with the boundary conditions as show in Table 1.

Table 1: Boundary Conditions for Primary Heat Exchanger.

	Units (USC)		Units (SI)	
CO_2 Inlet Temperature	°F	779	°C	415
CO_2 Outlet Temperature	°F	1112	°C	600
CO_2 Flow Rate	lb/hr	43640	kg/s	5.5
CO_2 Operating pressure	PSIA	2955	MPa	20.37
Pressure Part Design Pressure	PSIA	3975	MPa	27.41

The selection of the process heat exchanger's design temperature aimed to eliminate the necessity for utilizing nickel alloys. Studies indicate that, despite the higher power cycle efficiency achievable at temperatures greater than 600degC, the incremental expense of nickel alloys do not justify the associated investment [15]. The design pressure was selected based on conditions representing typical sCO_2 power cycles and was defined prior to finalizing these application specific operating conditions. High design pressure provides margin on operating temperatures

for pressure parts. Figure 7 shows the relationship between the design pressure and the allowable tube midwall temperature for the PHX tubes.

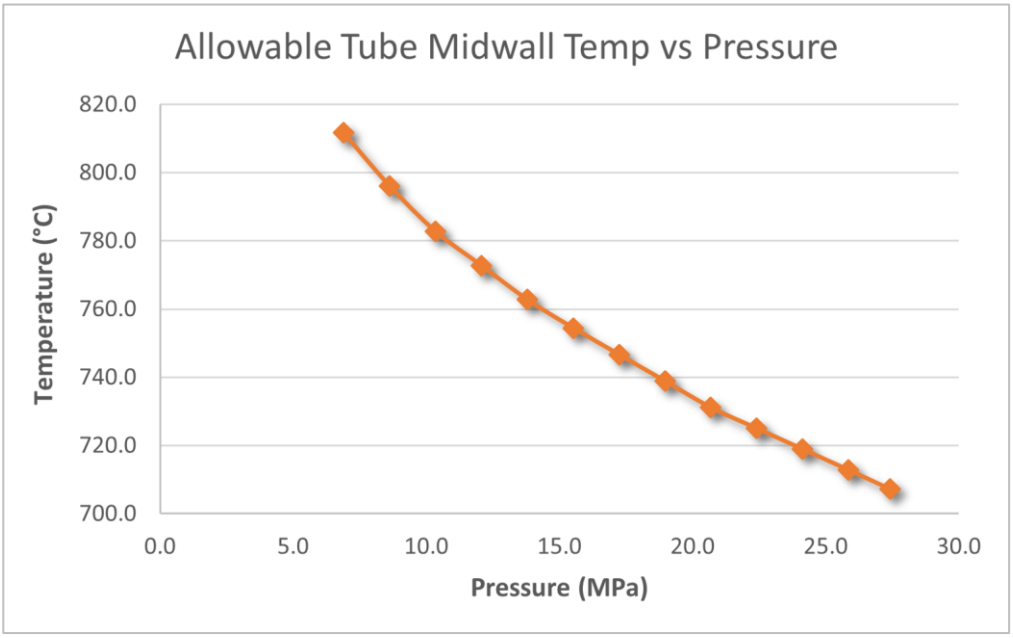

Figure 7: Allowable Tube Wall Temperature vs Design Pressure.

sCO_2 cycle efficiency can be maximized by minimizing pressure losses within the various components between the pump and the turbine. While there was no turbine in this test setup, the PHX was designed to maintain a minimal pressure drop. A challenge with low pressure drop is flow distribution, and calculations were done to ensure the flow through each tube would be within an acceptable range. Valves were included to allow the pressure drop to be adjusted, these valves will be discussed in more detail in the controls section of this paper.

Surface Layout and Design

There are several significant differences when laying out heat transfer surfaces for sCO_2 applications as compared to water/steam. The first challenge is the overall temperature range seen in an sCO_2 PHX is much lower than that of typical water-based boilers. The high inlet temperature of the sCO_2 means that there is a strict limit on the overall efficiency of the PHX, as the flue gas exit temperature cannot be dropped easily. To maximize this efficiency to the extent possible, we elect to place the coldest fluid at the exit of the system where it will best cool the flue gas. The higher temperature CO_2 is then routed through the remaining surfaces. This means the higher fluid temperatures coincide with higher heat fluxes and require careful consideration of materials for each heat transfer element.

The second challenge associated with sCO_2 systems is the lack of phase change within the PHX. Where in a typical steam boiler, the designer can leverage latent heat of vaporization within the furnace walls to maintain a steady working temperature, in the sCO_2 designs all surfaces experience changing fluid temperatures. To determine the routing of the fluid through these surfaces, considering any high radiant flux areas near burners or early convective elements must consider the properties of the fluid across the expected load range.

Designing pressure parts as a retrofit into an existing unit comes with inherent limitations on the amount of surface and the possible layout of that surface. Overall efficiency of the heat exchanger was reduced from what would be expected in full scale unit due to the limited space available. As part of this project, we wanted to verify performance of surface layouts expected in future larger scale deployments, so flat radiant panels and typical convective tube bundles were considered.

Considering overall efficiency, and heat fluxes, the PHX pressure parts were designed with the fluid inlet at the far end of the furnace away from the burner. Figure 8 shows the flow of CO_2 through the system. The fluid flows through a convective element, maximizing heat transfer and efficiency of overall heat pickup. The sCO_2 then flows through radiant panels that sit on the sides of the furnace. The furnace floor and roof were not included in the radiant surface due to the horizontal layout of the furnace. The floor of a coal fired unit is expected to fill with ash, and surface in this region would be difficult to characterize over time and interfere with cleaning of the unit. The roof was not included to avoid flame impingement and unacceptable heat flux if the flame rises towards the roof of the unit which is typical for horizontal burner installations.

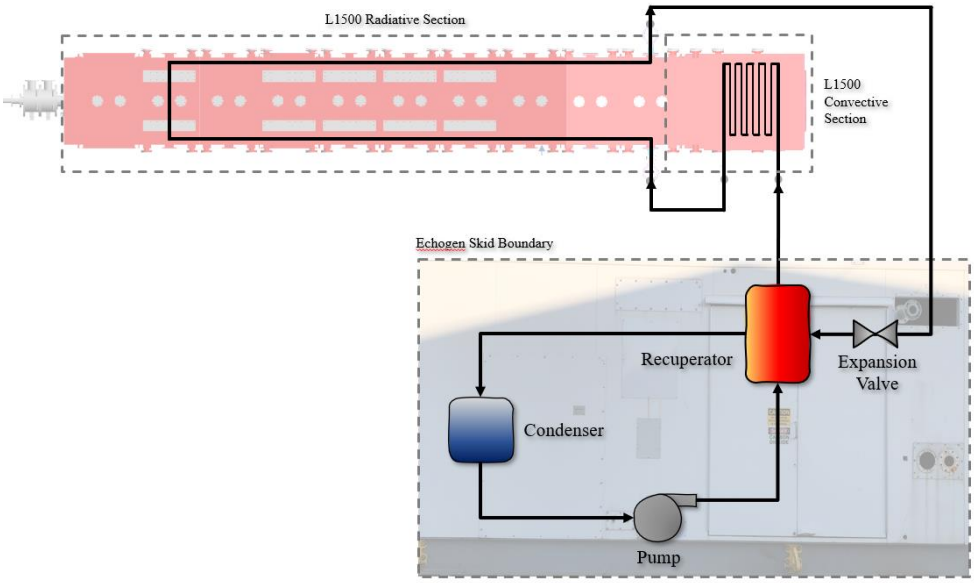

Figure 8: Schematic of the sCO_2 flow through the Echogen skid and the L1500. The expansion valve mimics the effects of a turbine in the Brayton cycle.

Material selections for this unit were made to handle both the high temperatures and pressures expected within a typical sCO_2 system. Previous design efforts in sCO_2 indicated that all high temperature surfaces will be using advanced metallurgies, up to and including nickel alloys for some applications. For this test project the sCO_2 outlet conditions were kept to 600°C, allowing us to avoid the expensive nickel alloys in favor of stainless materials. Super 304H was selected for the pressure parts, as it has better stress characteristics at high temperatures than the majority of comparable materials without going to nickel alloys. Figure 9 shows a comparison of materials considered for sCO_2 projects.

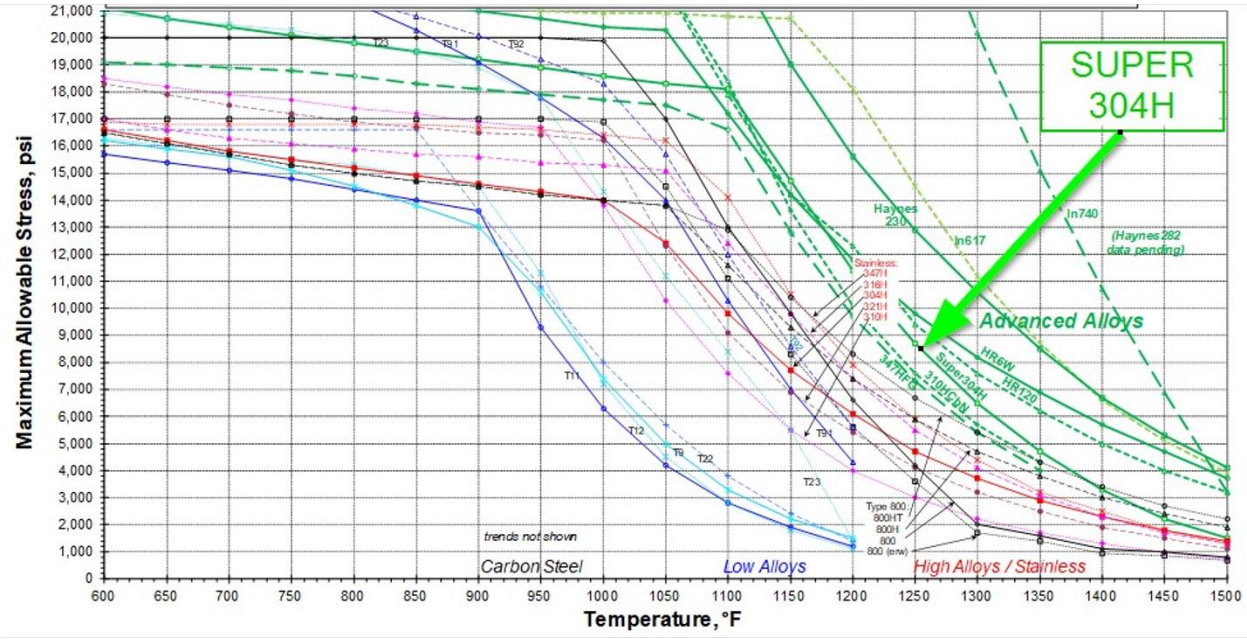

Figure 9: Comparison of Material Strength for high pressure and temperature applications.

PHX Controls and Instruments

The majority of control systems are outside the scope of the PHX. The only control items within the PHX are flow balancing valves located at the inlet to the radiant section. This allows the operators to redistribute flow to any tubes that may be operating hot due to uneven flux on the tubes. By design, there is a low overall pressure drop through the radiant surface. Without sufficient differential pressure there is a risk of imbalance in the flow, which may result in overheating of specific tubes. This is particularly likely at low flow rates, where the valves will be manipulated to increase the overall differential pressure as required. It should be noted that the flow balancing valves are included in this unit for experimental purposes to understand the effects of uneven flow distribution. Commercial applications of this technology would not incorporate these valves into the packaged solution.

Tube metal temperatures are critical for this evaluation unit, both to protect the pressure parts from overheat failure, and to verify predictions vs actual performance. To provide this information the PHX was instrumented more heavily than production units would be. This included tube skin thermocouples on every tube at the outlet of the convective and radiant elements. A general arrangement drawing of the skin thermocouple can be found in Figure 10. The tube skin thermocouples allow for individual tube calculations to be performed, helping to verify overall flow balancing and tube to tube flux discrepancies. While testing, these measurements will assist operators in evaluating the need for flow adjustments and in detecting factors related to flame location and varying fluxes within the furnace.

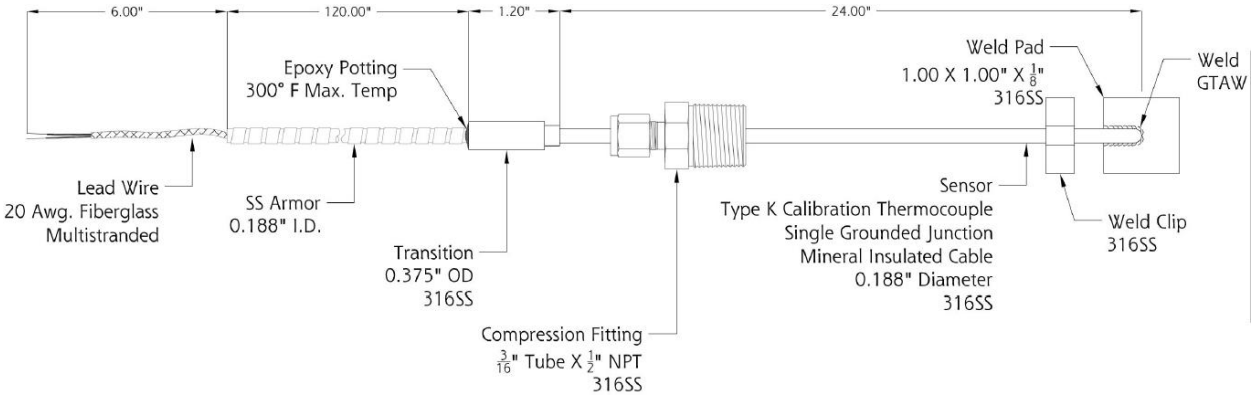

Figure 10: Tube Skin Thermocouple Schematic

Additionally, heat flux sensors, configured as an array of thermocouples, are embedded in the tube walls near the surface as well as near the mid-wall, as shown in Figure 11. The flux sensors are located at 6 locations within the furnace as shown in Figure 12. By observing the temperatures near the tube surface and mid-wall, the heat flux can be calculated at each location based on the tube metal thermal conductivity. The temperature readings can be used directly by operators to determine if there is a risk of overheating the tubes at critical locations within the furnace, while the flux readings are used to verify performance of the thermal modelling done during design.

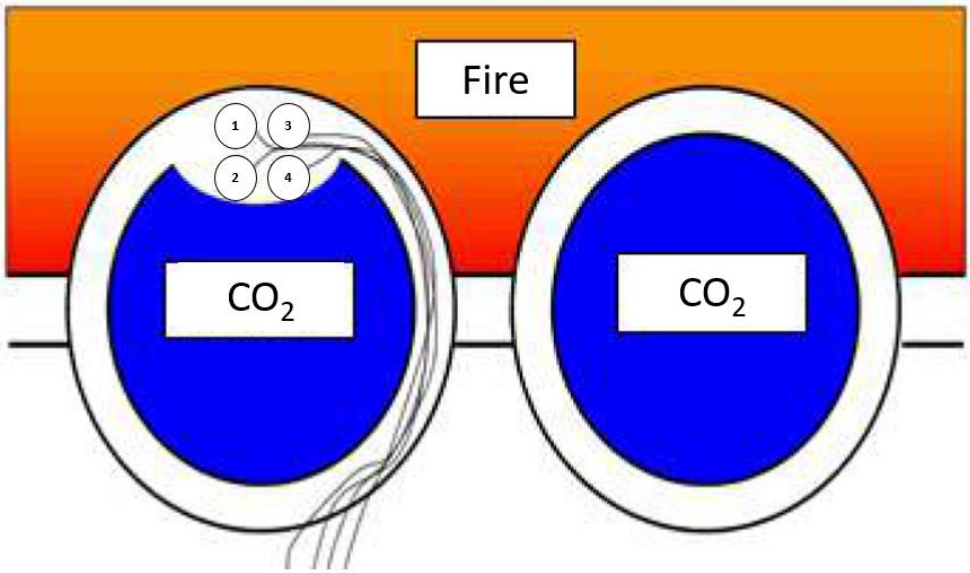

Figure 11: Flux Sensor TC Layout Concept.

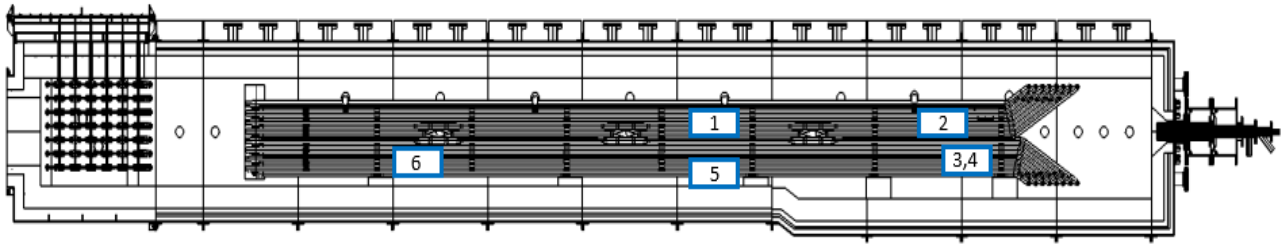

Figure 12: Heat Flux and Radiant Tube Skin Sensor Locations on the Primary Heat Exchanger. Note, sensors 3&4 are at different elevations.

Flux sensors were located on both walls, with three sensors being placed down the length of the furnace, and three sensors being placed close to the burners. Tubes near the burner are likely to receive high heat flux that may result in overheating. The higher sensor concentration in this region can detect if this is occurring and allow operators to reduce heat input or increase sCO_2 flow rates to cool these tubes.

It was predicted that at full load, even with maximum sCO_2 flow, the tubes near the burner may experience higher than allowable metal temperatures. If the flux sensors verify this behavior, insulation will be placed over the tubes where they cross from the left to right wall of the furnace.

The Furnace Model

Reaction Engineering International (REI) updated and refined its existing Computational Fluid Dynamics (CFD) model of the L1500 pilot furnace to include a detailed description of the initial design concept of the sCO_2 primary heat exchanger (PHX). Design drawings of the heat exchanger provided by project partner Riley Power include a radiant section extending from near the midpoint of section 2 to the midpoint of section 10 as well as in section 12 of the furnace. The part of the heat exchanger in section 12 will be referred to as the convective module of the PHX. It should be noted that this is different from the convection section of the L1500, which has been defined earlier. A representative CFD model of the furnace and the PHX including the radiant and convective modules were developed for this program. Components of the initial design were previously identified in Figure 5.

The REI CFD model has been extensively leveraged to evaluate the configuration of the heat transfer surfaces and to determine the best practice operating conditions that will approach the design value of heat transfer to the Echogen sCO_2 Thermal Management System (1.26 MW) and to maintain the tube metal heat flux below a threshold for concern about material performance (175,000 W/m^2). REI simulated 12 scenarios that have exercised both operational and configuration variables expected to impact the total heat transfer and the peak heat flux to the heat exchanger surfaces.

Prior to the retrofit with the PHX, the L1500 had mostly been operated at a firing rate in the 3.0 to 3.5 MMBtu/hr (0.87 – 1 MW) range to best stabilize refractory temperatures at a steady condition throughout operation. However, the furnace was designed to be operated at 1500 kW which corresponds to approximately 5.12 MMBtu/hr. Upon installation of the primary heat exchanger (PHX) it is known that the furnace will require a higher heat input to achieve the same temperatures in the L1500 due to the heat removal by the PHX. It was decided to assign the baseline condition at 3.0 MMBtu/hr because of the vast experience and data at those conditions.

The baseline condition was essentially taken from an existing model with only the addition of the PHX.

The first parametric was used to determine the impact of air staging on heat distribution and was identical to the baseline case in every other way. Parametric cases 2 through 11 were all performed at a firing rate of 6 MMBtu/hr (1.76 MW), which was determined to provide nearly the required heat transfer to the PHX. Table 2 provides a summary of the CFD cases, the operational conditions that were varied, and the purpose of each variation. The operational variations included: burner stoichiometric ratio (BSR, a reflection of air staging), theoretical excess O_2, fuel type (coal or coal and natural gas blend), swirl setting of the inner and outer secondary registers (swirl), and the introduction of a bluff body (BB) in the burner. The geometry of the heat exchanger was also evaluated by examining impacts of extending the PHX toward the burner in order to determine if additional surface area would be useful in moderating peak incident fluxes to heat exchanger tubes.

Table 2: Summary of CFD cases of the L1500 with Respective Study Purpose.

CFD Case Id.	Variations from Baseline	To determine the impact of _____ on heat removal & flux
Param1	FR=3, BSR=0.9	staged combustion at baseline firing rate (FR)
Param2	BSR=1.16, O_2=3	realistic firing rate (new baseline)
Param3	BSR=0.9, O_2=3	staged combustion at realistic firing rate and excess air
Param4	BSR=1.24, O_2=4	realistic FR with additional air
Param5	BSR=1.16, 95/5 Coal/NG	5% of fuel heating value from natural gas
Param6	Extend PHX toward burner	removing heat earlier from the system
Param7	swirl=0.3	reducing swirl to extend flame
Param8	BSR=0.8	staging more deeply
Param9	BSR=0.8, swirl=0.3	reducing swirl and staging more deeply
Param10	BB	introducing a bluff body to increase fuel velocity
Param11	BB, BSR=0.8, swirl=0.3	Increased fuel velocity, deep staging and reduced swirl

CFD and PHX Design Results

Impact of Increased Firing Rate

The impact of increasing the firing rate from the typical condition (3 MMBtu/hr) to a realistic condition for approaching the desired total heat transfer (6 MMBtu/hr) can be determined by comparing the Baseline case with Param2. Param2 produced very desirable results because it increased the heat transfer while having minimal impact on peak heat flux. Figure 13 provides a comparison of the predicted gas temperatures between these two conditions. It can be determined from Figure 13 that hot temperatures persist at greater axial positions relative to the burner with the increased firing rate, but there is little increase in peak flame temperatures. This

is supported by comparing the average temperature versus axial position plots for each of these cases, which is presented in Figure 14.

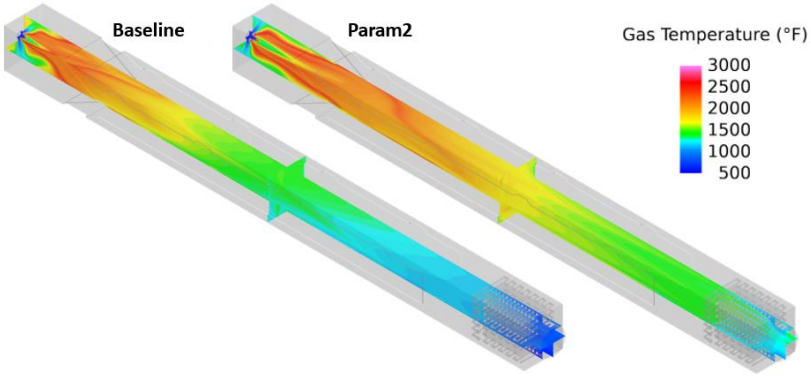

Figure 13: Comparison of predicted flue gas temperatures between the Baseline CFD model (3 MMBtu/hr) and the Param2 CFD model (6MMBtu/hr).

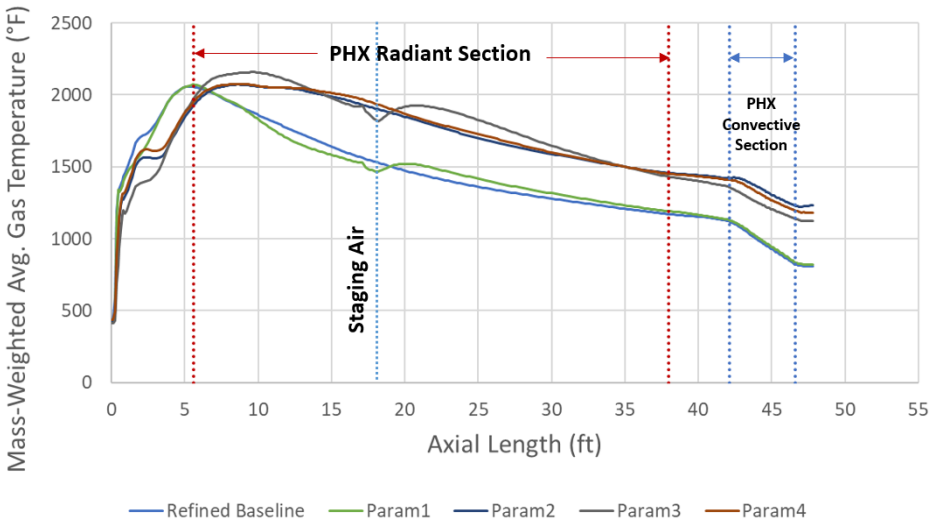

Figure 14: Predicted average temperature vs. axial position for the CFD cases baseline through Param4.

The predicted impact of the change in firing rate is depicted in Figure 15, which is a map of the heat flux as a function of location on the PHX. This figure shows that the peak heat flux is on the top and bottom cross members for the baseline case. The peak heat flux is predicted to be in the same place when doubling the firing rate, but also extends down the left and right walls. It is hard to discern a difference in the absolute value of the peak heat flux between the cases from this plot, but it appears similar.

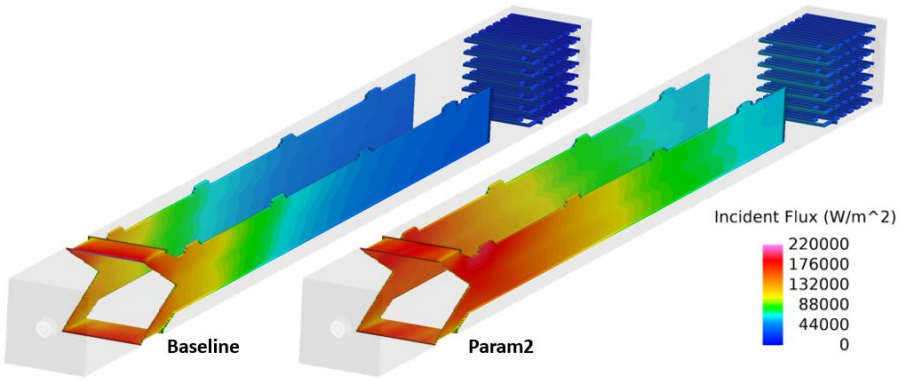

Figure 15: Map of heat flux as a function of position on the PHX for the baseline and Param2 CFD models.

The predicted CFD data were examined to determine the peak heat flux and total heat removal to the PHX in the Baseline and Param2 CFD cases. These data are presented in Table 3. These data show that there is a decrease in peak heat flux when doubling the firing rate. This may seem counterintuitive, but there was also one other variable that changed simultaneously, which was the excess air. The higher firing rate case was run at 3 vol% O2, dry whereas the 3 MMBtu/hr case was run at 2.2 vol% O2, dry. The impact of regional stoichiometry appears throughout these results and proves to be an important variable.

Table 3: Predicted peak heat flux and total heat duty of the PHX for the baseline (3 MMBtu/hr) and Param2 (6 MMBtu/hr) CFD models.

	Units	Baseline	Param2
Total Duty to PHX	MW	0.632	1.143
Maximum Inc. Heat Flux to PHX	W/m^2	218,000	196,000

Impact of Burner Swirl

One of the concepts investigated to reduce the peak heat flux to the PHX was to change operating conditions in such a way that the flame would be longer and extend the heat release profile. One way to do this is to reduce the tangential velocity of the air injected through the inner and outer secondary registers or reducing the swirl. Delayed mixing of the fuel and air and the expectation is that the heat release from the flame is stretched through a longer axial portion of the furnace. Comparison of the results from the CFD cases Param2 and Param7 investigates this concept.

A comparison of the gas temperature profiles these two cases indicates that the flame sheet is indeed narrower near the burner for the reduced swirl case (Param7) as expected. However, peak temperatures are hotter, and gases mix rapidly in sections of the furnace that are most prone to the highest heat fluxes. While these behaviors were not desirable or expected, they can easily be explained. In the near burner regions where the gases are obviously more stratified, the gases are not mixing well with the fuel as intended. This does delay the heat release, but it also causes substoichiometric combustion locally. Without the necessary air available for combustion and to accept the energy from the reaction, the adiabatic flame

temperatures are higher. In addition, the jet-like introduction of the reactants through the burner causes high shear with the stagnant gases near the wall, eventually producing good mixing and heat release near the walls with heat fluxes that are much greater in magnitude for case Param7.

Impact of Staging

Staging the flame by introducing a portion of the air through over-fire air ports was investigated as a strategy for extending the heat release profile of the flame to reduce peak heat flux to the PHX. Model predictions showed that staging the burner does produce an elongated flame. The conditions that stretch the flames bring benefits to alleviating high heat fluxes to the front end of the radiant section. However, as the fuel and oxidant mix further downstream, local stoichiometric ratios produce regions of higher peak temperatures in the staged cases. The undesirable effects of this are compounded by the reduced amount of nitrogen (due to decreased burner air), which acts as a heat absorbing diluent. These compounding factors result in an increase in peak incident flux to the PHX under staged conditions and a trend of higher maximum incident fluxes with decreasing burner stoichiometric ratio.

Impact of Bluff Body

Geometrical changes to the burner and the heat exchanger itself were also examined. Changes to the burner entailed the addition of a bluff body in the center of the coal nozzle. The bluff body is a 0.5" OD pipe that acts to convert the coal nozzle into an annular opening. The objective of the bluff body is to increase primary air and coal particle velocities such that mixing, and heat release are extended over a greater length than they would otherwise. Like other efforts to extend the heat release profile of the flame, this effort had an undesired impact on peak heat flux to the PHX. The higher velocity of the primary stream likely increases the shear between that stream and surrounding streams which in turn increases mixing.

Impact of Extended PHX Surface

The geometry of the heat exchanger was also evaluated to determine if additional surface would be useful in moderating the peak incident fluxes and bringing the heat fluxes to more acceptable levels. To that end, REI completed a simulation that involved extending the heat exchanger an additional 2 ft toward the front wall. The hypothesis being that additional surface area would alleviate the high heat fluxes by spreading the heat absorbed over a larger surface. In the preceding report, the simulation of PHX expansion was a preliminary scoping case. Since that time, Param6 was run to completion with identical operating conditions as Param2 with a firing rate of 6 MBtu/h, unstaged combustion and 3% excess O_2 dry. As shown in Figure 16, the peak heat fluxes have decreased as a result of the PHX expansion with a decrease of nearly 6% from the Param2 maximum. The color contours in the figure indicate the decrease in radiant flux to the leading edge of the tubes along the floor and roof of the furnace as well as to the surfaces along the sidewalls nearest the burner.

As shown in Table 4, peak heat flux in Param6 is lower than Param2 with little impact to the overall duty to the PHX. The predicted peak heat flux occurring at the crossmembers of the PHX is 185,000 W/m^2, which is still above the target level of 175,000 W/m^2. However, this design change provides a notable improvement to reduce peak heat fluxes over the other means examined in the parametric cases. Through subsequent discussions within the team, it was determined the design modeled in Param6 would the design selected for installation and that relatively straightforward strategies can be employed during installation to help to further regulate peak fluxes to the crossmembers.

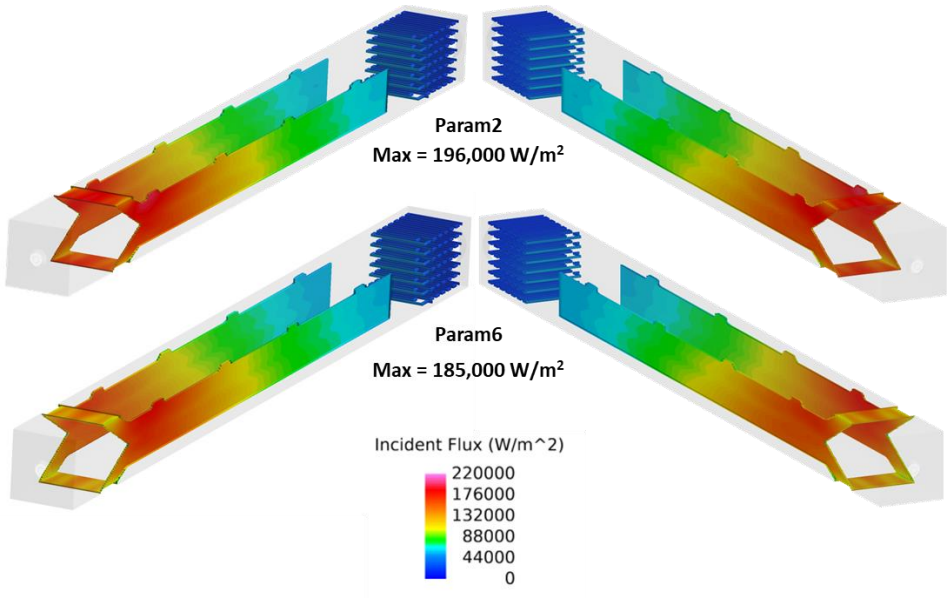

Figure 16: Incident heat flux profiles showing the decrease in peak heat flux due to expansion of the PHX surfaces.

Table 4: Tabulation of total duty to the PHX along with the maximum incident heat flux prediction.

	Units	Param2	Param6
Total Duty to PHX	MW	1.143	1.135
Maximum Inc. Heat Flux to PHX	W/m^2	196,000	185,000

Impact of Natural Gas Flame

The L1500 will run on a 100% natural gas flame for periods of time. Param6 is modified to run on 100% natural gas to predict how this scenario will differ from a coal flame. Table 5 shows the conditions used in the Param6 and modified Param6 models.

Table 5: Operating conditions for the Design Case compared to running a 100% natural gas flame.

	Units	Param6 (Design Case)	Param6_Nat_Gas
Description		**Unstaged, Excess O_2 = 3% Dry**	**100% Nat. Gas based on Design Case**
Firing Rate	MBtu/hr	6.0	6.0
Coal Flow	lb/hr	476.0	N/A
Natural Gas Flow	lb/hr	N/A	261.9
Primary Air Flow	lb/hr	863.8	N/A
Primary Temperature	°F	106	N/A
Primary Velocity	ft/s	67	N/A
Inner Secondary Air Flow	lb/hr	1513.5	2508.6

Inner Secondary Temperature	°F	500	500
Inner Secondary Velocity	ft/s	114	188.8
Outer Secondary Air Flow	lb/hr	2874.8	2508.6
Outer Secondary Temperature	°F	498	498
Outer Secondary Velocity	ft/s	178	155
Staged Air Flow	lb/hr	N/A	N/A
Staged Air Temperature	°F	N/A	N/A
O_2 Concentration	% Vol, Dry	3.0	3.0

Operating the unit with 100% gas is predicted to significantly increase heat fluxes at the near-burner end of the radiant section of the PHX. The increase in heat flux is consistent with the faster heat release of combustion with gas fuel versus coal. This leads to a significant increase in peak tube metal temperatures from 1100°F for coal to 1400°F when firing gas. In addition, the predicted heat transfer to PHX increases more than 10% as shown in Figure 17.

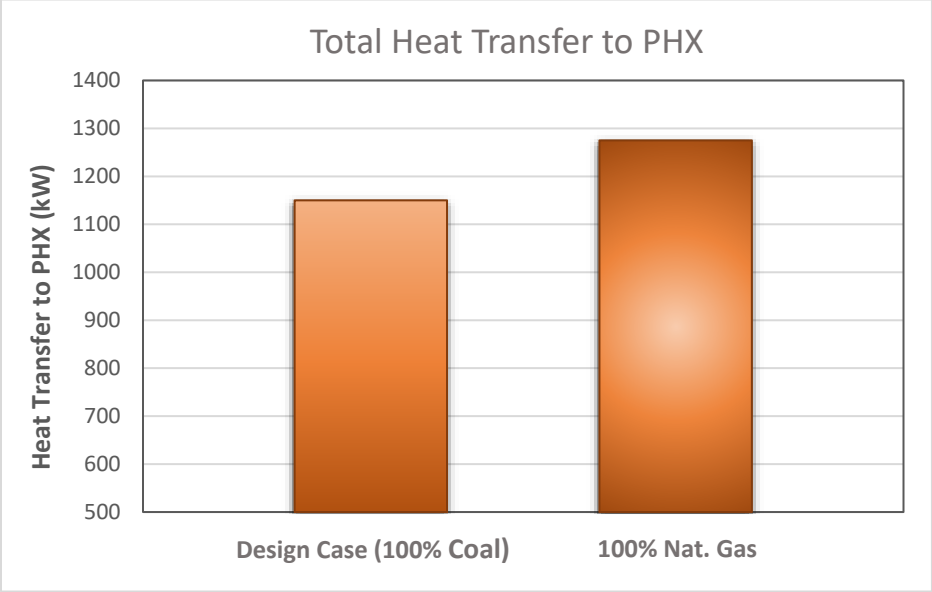

Figure 17: Comparison of heat transfer to PHX for coal versus gas at 6 MBtu/h firing rate.

Heat Flux and Tube Metal Temperatures

Figure 18 shows predicted heat flux throughout the PHX. High heat flux is noted near the burner end of the furnace with a magnitude approximately 4 times larger than the radiant exit. The fluid is heated throughout the radiant, and with roughly even flux on each wall, the sCO_2 is heated roughly halfway at the burner end, leading to elevated metal temperatures which are worsened by the high flux in this region. This can be seen in Figure 19 which shows predicted fluid and tube mid-wall temperature through the length of a typical radiant tube.

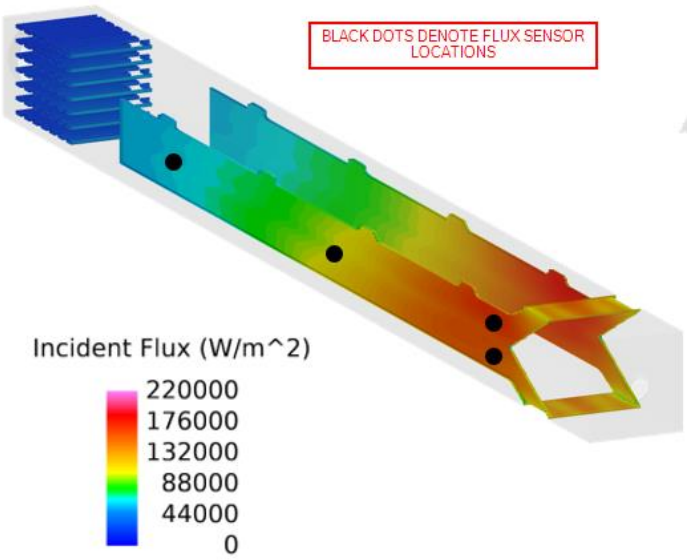

Figure 18: Predicted Heat Flux Profile (CFD).

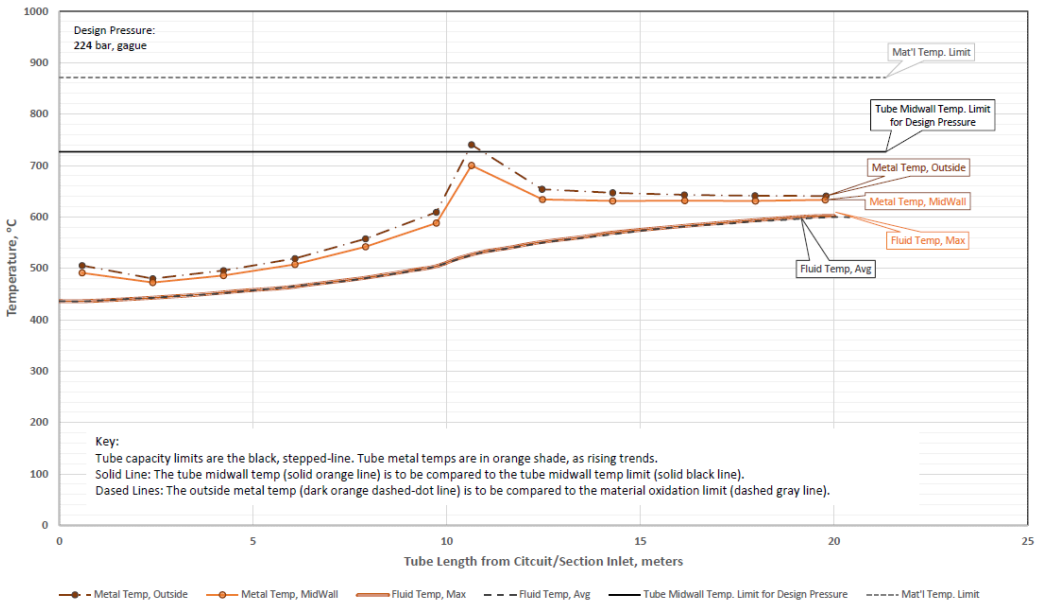

Figure 19: Predicted Radiant Tube Metal Temperatures as a Function of Tube Length from Radiant Section Inlet.

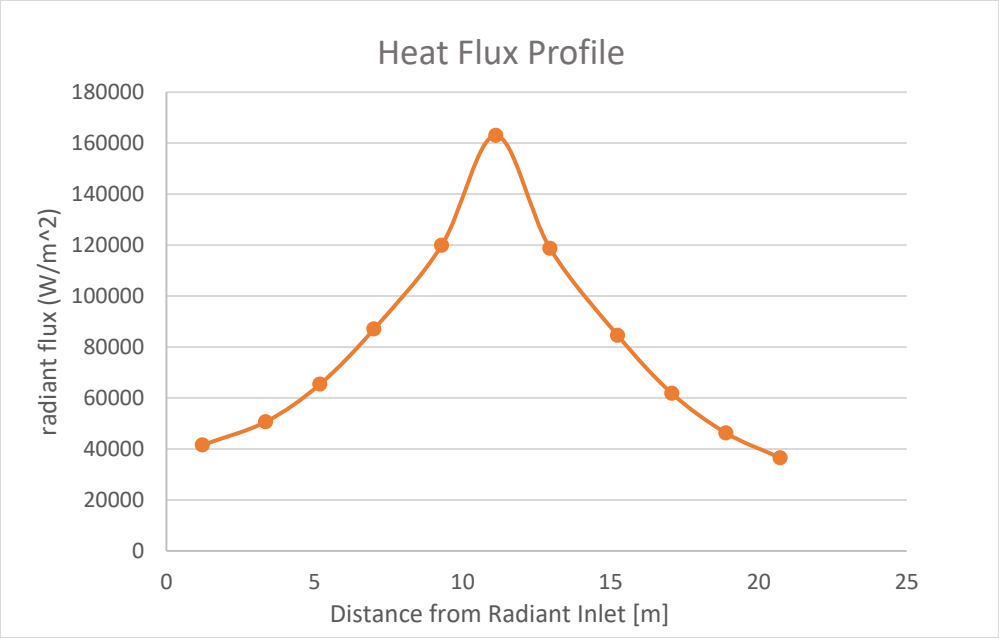

Figure 20: Predicted Heat Flux Profile (Transient Model) As a Function of Distance from Radiant Inlet.

The peak metal temperatures at the location of maximum flux drives the material selection and wall thickness required for the radiant elements. The curve shown in Figure 20 has a peak flux of 161,000 w/m^2. This was considered the maximum acceptable flux for the system to operate at the design pressure. As the operating pressures achieved during early testing are significantly lower than the base design, this provides substantial margin, letting the unit operate with higher fluxes than originally specified. This negates the need for insulation materials to protect the tubes in this region, as discussed in the design section of this paper.

Ideally one could use a colder fluid near the high flux region of the furnace, but for this unit this resulted in unacceptable routing of pressure parts which increased costs, or unacceptable flow rates through the radiant pressure parts, which result in insufficient cooling and worsen the issues. It is anticipated that larger units will also experience local high flux near burners, which are generally located some distance up any furnace walls. In both this and larger scale units, refractory or other shielding materials may be employed to limit flux directly around the burners. Depending on the size of the unit and the heat source, alternative geometry can be used to keep hot fluid away from high flux regions.

The CFD results show that there are concerns with overheating the PHX in the regions near the burner. The PHX is extended closer to the burner from the initial design to reduce the peak heat flux. Efforts to reduce the peak heat flux by manipulating the heat release profile of the flame are counterproductive due to regions of sub-stoichiometric conditions which leads to elevated adiabatic flame temperatures. Increasing the amount of excess air is the only operating condition available to reduce the peak heat flux.

L1500 Testing

Experimental Procedure

After the design, fabrication, and installation of the PHX in the L1500 and integration with the sCO_2 Thermal Management System, testing occurred to evaluate the performance of the

PHX. Natural gas and western US bituminous coal were used as the fuel in these tests. Results of the proximate and the ultimate analysis of the coal used are shown in Table 6.

Table 6: Proximate and Ultimate Analysis of Coal

Component	**Mass fraction / Heating value**
Moisture (%)	3.12
Ash (%)	8.50
Volatiles (%)	41.24
Fixed Carbon (%)	47.14
Sulfur (%)	0.83
Carbon (%)	71.75
Hydrogen (%)	4.94
Nitrogen (%)	1.54
Oxygen (%)	9.32
Heating Value (kJ/kg)	30319

A maximum thermal energy release of 1600 kWth was targeted. The primary air-to-fuel ratio was maintained at around 1.8-1.9. Inner and outer secondary air was introduced through individual swirl registers and their ratio was maintained at approximately 30/70 by mass. Around 4-5% excess oxygen in the dry flue gas was also targeted. A California Analytical Instruments (CAI) ZPA gas analyzer was used to analyze the flue gas. The analyzer was configured to detect CO2, CO, NO, and SO2 using the non-dispersive infrared absorption method (NDIR) and O2 using the paramagnetic method.

Before initial operation of the L1500, the CO_2 system undergoes nitrogen purging to eliminate residual moisture from hydrotesting and other maintenance related activities. When starting the L1500 operation, preheated secondary air is circulated through the furnace to gradually warm up the refractory, preventing thermal shock and simplifying inventory control. Once the PHX is sufficiently heated, the system is charged with CO_2 and flow through the PHX is established. System temperatures are allowed to stabilize at which point the natural gas flame is initiated. The firing rate is slowly increased to manage the heat rate of the refractory. For reference, prior to installing the PHX and sCO_2 system, the furnace was heated over a five-day period to get the refractory hot enough to fire coal. When the system reaches an acceptable temperature profile, coal is introduced. This process takes place incrementally while reducing the natural gas flowrate until the desired fuel ratio is achieved at the target firing rate. At this point, the test matrix may be performed.

Following testing activities for the day, the flame is transitioned to a 100% natural gas flame at a reduced firing rate so that the system can safely remain heated while operators are not on site. Similarly, at the end of the test campaign, the flame is transitioned to a 100% natural gas flame and the firing rate is slowly decreased until no fuel is fed into the system. The air preheaters are turned off and the maximum airflow is fed to the furnace to increase cooling. CO_2 flow is eliminated once the PHX can be safely cooled from only the air flow. The system is allowed to cool for several days and then the airflow is eliminated.

Campaign 1 (05-30-23 through 06-02-23)

During the first week of testing, there were challenges with getting the furnace to operate at the design test conditions. One challenge was managing the furnace temperature. This furnace is refractory lined. In this configuration, the hot refractory (~ 2500 °F near the burner) radiates back to coal particles, heating and igniting them. This behavior replicates multiple coal

burners in an array, radiating to each other, like in an industrial system. In the new furnace configuration, it is not possible to get the refractory walls hot at low firing rates because of the relatively cool PHX surface. This enabled the furnace to come up to a high firing rate, much more quickly, but it also made it more difficult to stabilize a flame. There were many instances of blowing off the flame. To overcome this difficulty, the right amount of air preheat (even with gas firing) and secondary burner register swirl were critical. Additionally, the observation was made that coal burnout was likely lower than expected during this test run.

Despite the difficulties, the team successfully ran the Thermal Management System for approximately 100 hours. A fuel blend of 80% coal, 20% natural gas was reached at a firing rate of 1.6 MW as shown in Figure 21. It was determined that a firing rate of 1.6 MWth was the ceiling of operation due to limitations in both the induced draft and forced draft fans. To increase the thermal heat input, the amount of air would need to be increased to achieve a stoichiometric reaction. The accompanying fuel flow rate distribution is displayed in Figure 22 for reference.

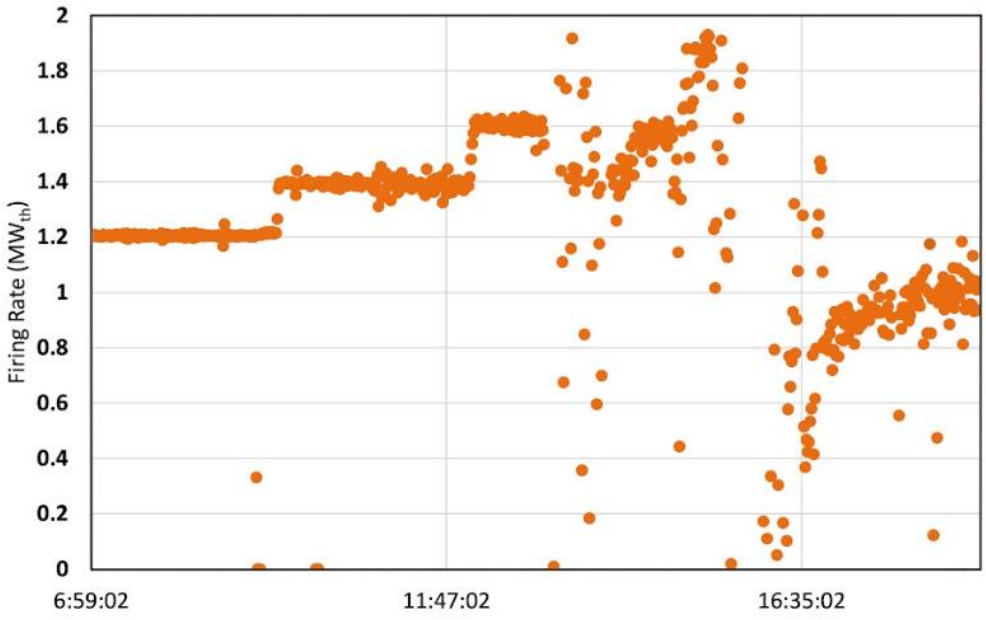

Figure 21: Combustion system firing rate 05-31-23.

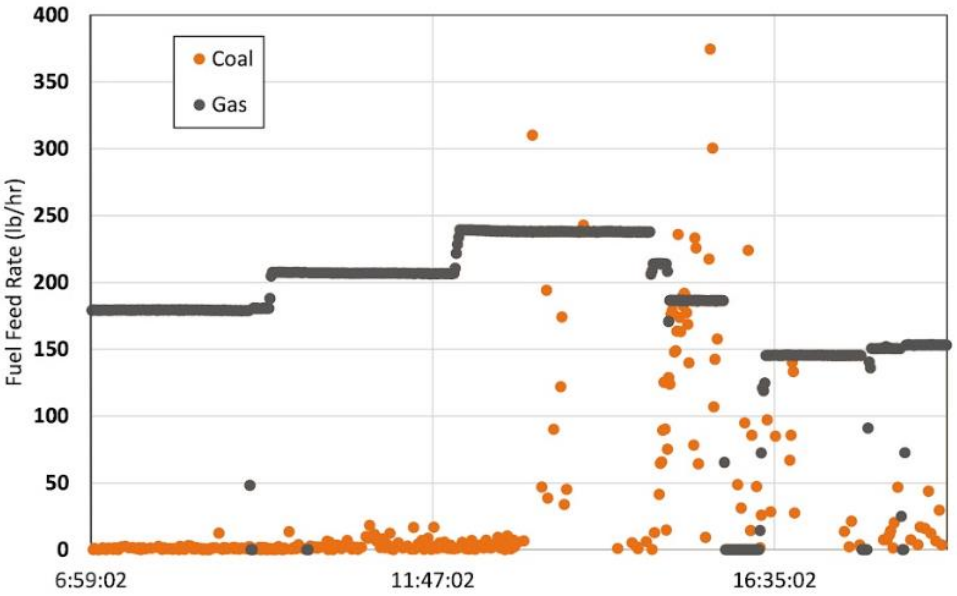

Figure 22: Combustion system fuel flow rate 05-31-23.

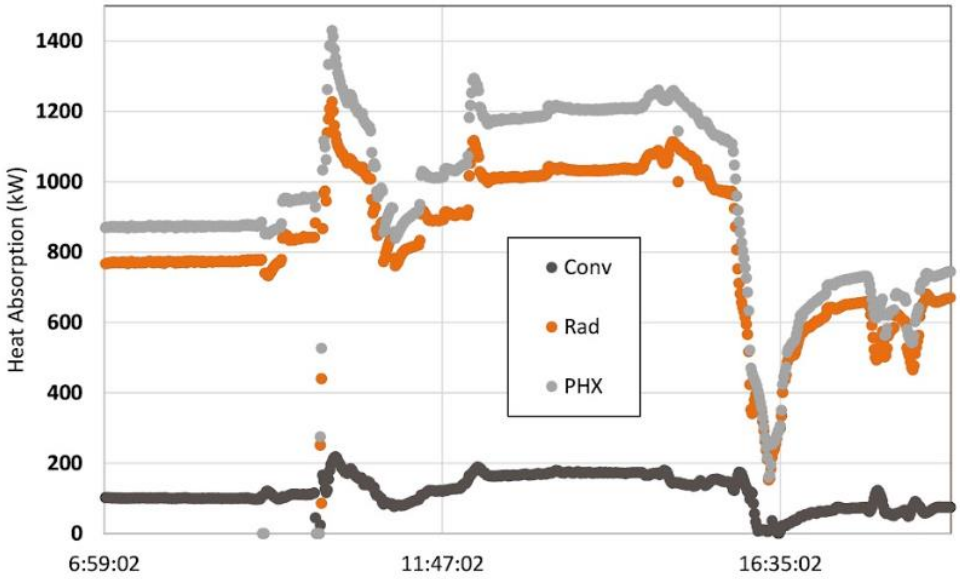

Figure 23: PHX heat absorption 05-31-23.

Although the data set is largely transient, its significance lies in the magnitude of heat absorption in the PHX. Focusing on the mid-span of the data set, before the switch was made to coal, the furnace was operating at 1.6 MW on a natural gas flame. This corresponds to a heat absorption in the PHX was 1.2 MW, which was the only time in the two test campaigns where we reached the design heat absorption conditions. These conditions are presented in Figure 23. Conclusions made from the data analysis show that ash buildup on the PHX is responsible for

reducing the heat absorption. The increased amount of ash produced a thicker layer on the radiant section, leading to higher thermal resistance and a subsequent decrease in the overall heat transfer coefficient of the PHX. Consideration for ash build-up were made during the design phase of the PHX. The analysis led to the addition of mechanical vibrators on the convective module, where the effects were predicted to be most significant. Prior to the installation of the PHX, the furnace returned between 3-5% unburnt carbon in ash, while a post-test analysis of the retrofit installation produced 15.2% unburnt carbon.

Observations during testing indicated that the recuperator (RHX) was underperforming. Elevated temperatures at the low-pressure outlet coupled with reduced temperatures at the high-pressure outlet suggested that the recuperator performance was compromised. Additionally, pressure losses across both side of the RHX were higher than design. Welding procedures and debris from field erected piping were identified as potential contributors to the performance issues. In the days following the campaign 1 testing, the Thermal Management System was dismantled, and the recuperator was backflushed for several days. Results from this procedure were positive allowing for higher temperature operation during test campaign 2.

Campaign 2 (06-19-23 through 06-22-23)

The data collected during the second week of testing showed that the system could achieve stable operation for long periods of time. During this test campaign the system was operated for an additional 100 hours. Testing was performed at different firing rates and fuel blends. Additionally, the system response to small changes in firing rate and excess air was investigated.

During this test campaign the heat absorption in the PHX hovered near 1 MW. However, the absorption did reduce slightly throughout the test campaign. This is a further indication that ash build up on the PHX over time is causing this reduction.

Comparison of Experimental Data and Models

PHX Efficiency and Firing Rates

Table 7 shows a comparison of the heat transfer model (as configured prior to testing) operating with similar overall boundary conditions to a set of data showing one of the highest absorptions in the test data. This shows the differences in predicted heat transfer performance in the radiant and convective sections of the furnace. The table also shows pressure measurements of the sCO_2 at various points throughout the system.

Table 7: Simulation vs Results.

		Model (Un-Tuned)	Results
sCO_2 Flow	kg/s	4.4	4.4
sCO_2 Inlet Temp	°C	350	349
sCO_2 Convective Outlet Temp	°C	387	379
sCO_2 Radiant Outlet Temp	°C	550	557
Convective Duty	MW	0.197	0.108
Radiant Duty	MW	0.882	1.005
Fuel Heat Input	MW	1.079	1.113
Combustion Air Heat Input	MW	0.12	0.12
Total Heat Input	MW	1.63	1.63
Efficiency	%	61.6	63.6
sCO_2 Inlet Pressure	MPa	14.36	14.42
sCO_2 Convective Outlet Pressure	MPa	14.01	14.10

sCO_2 Radiant Outlet Pressure	MPa	13.95	13.95
Convective Pressure Drop	MPa	0.35	0.32
Radiant Pressure Drop	MPa	0.06	0.15

A comparison of model-predicted heat transfer to the radiant and convective modules of the PHX is shown in Figure 24. There is good agreement between the model and the experimental data for the heat transfer to the radiant module. However, a significant difference exists between the model and the data for the convective section. The model shows nearly 2 times the amount of heat transferred to the convective module. Observations during the tests indicate that significant fouling of the convective tubes was occurring. Due to the fact that the degree of fouling is an unknown a priori for the CFD simulation, an assumed emissivity and thermal resistance are prescribed to the heat transfer surfaces. The assumed resistance accounts for a degree of fouling on the tube surfaces. The comparisons suggest that the assumed boundary condition prescribed to the radiant module agrees well with actual conditions in the furnace. However, the prescribed resistance for the convective tubes assumes cleaner surfaces than what was observed during the testing. REI's approach of coupling fireside and tube-side conditions using its CFD and process modeling tools provides a capability to compute sCO_2 exit temperature based on the CFD model's predictions of PHX heat duty. The impact of the difference in heat transfer to the PHX on sCO_2 exit temperature is shown in Figure 25. The near 30°F difference between the model's calculated sCO_2 temperature and the measurement is consistent with the difference in overall heat duty between the model and the measurements.

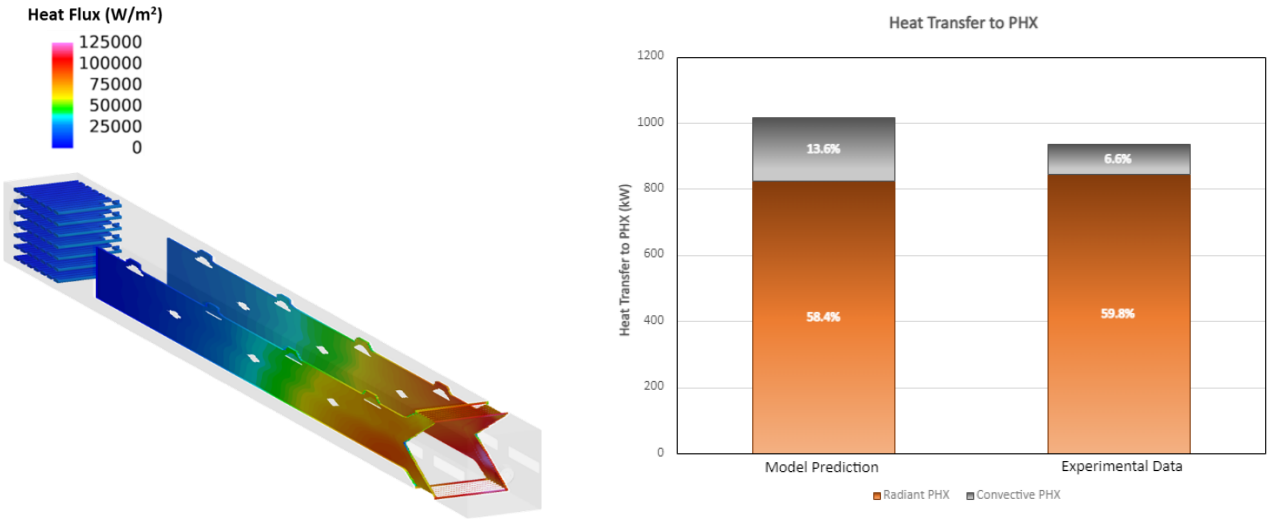

Figure 24: Comparison of model-predicted and measured heat transfer to the PHX. The significant difference in heat transfer to the convective module is indicative of the large degree of fouling of tube surfaces observed during the tests. The percentage of total heat input into the furnace absorbed by each heat transfer surface is provided.

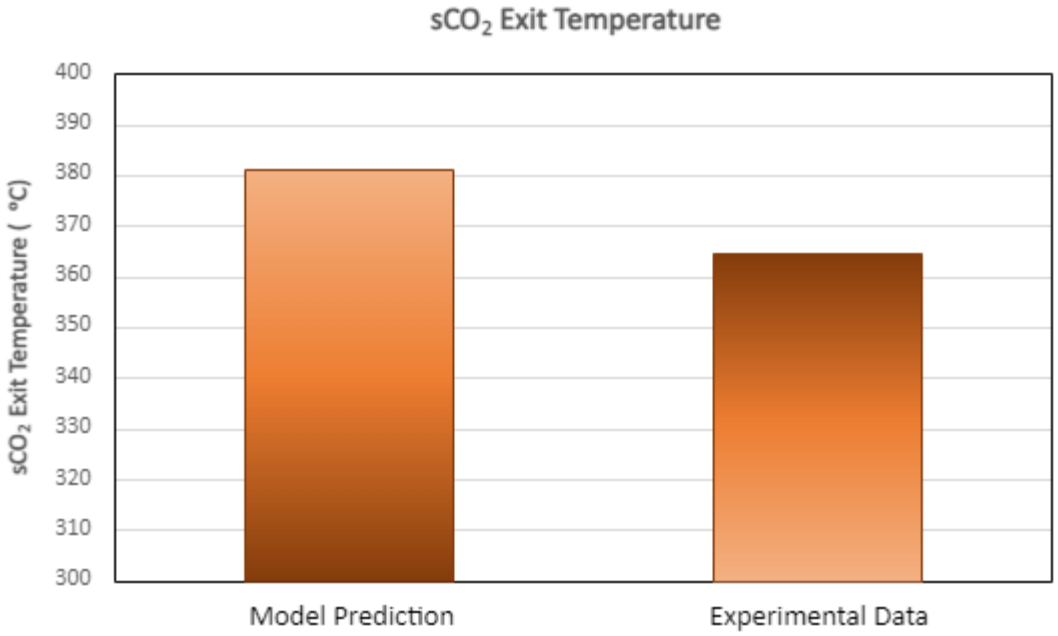

Figure 25: Comparison of sCO_2 exit temperature showing impacts of reduced overall heat transfer to the PHX in the experiments.

REI's approach is to modify the thermal resistance of heat exchanger tubes as availability of data allows in order to accurately capture the amount of heat absorbed. This approach has been successfully applied in REI's assessments of utility boilers to provide accurate descriptions of heat loss throughout the system and associated impacts on gas temperature, flue gas velocities, heat flux to furnace walls, gas and particle chemistry, and particle deposition. In future simulations of test conditions, this same approach will be applied, and a higher thermal resistance will be prescribed to the convective module to represent the impacts of the fouling observed in the early testing.

PHX efficiency can be defined as the amount of heat transferred from the fuel to the working fluid. In this case we calculate heat input based on the high heating value of the fuel and heat added to the combustion air from electric air preheaters. Heat transferred to the sCO_2 is determined by the change in enthalpy of the fluid between inlet and outlet of the PHX. During the design of the system this efficiency was calculated between 60-65% for this system. This is a low efficiency as compared to typical fired heaters, due to the high sCO_2 Inlet temperature, limited space available for convective heat transfer surface, and the lack of an air preheater to recover waste heat from the flue gas. Larger scale systems for sCO_2 have higher predicted efficiency. The data collected verifies the overall performance of the PHX, with an efficiency just above the predicted levels.

Using the predicted efficiency, to achieve full sCO_2 temperature at the design flow rate would require a total heat input of ~1.9 MW. This firing rate is substantially higher than the L1500 typically achieved, as the furnace typically operated without substantial heat transfer surface and was limited by furnace exit gas temperatures into the baghouse and other equipment. With the PHX installed, the system was able to achieve peak heat inputs of 1.63 MW from fuel and 0.12MW using an external electric air preheater. The limiting factor during test firing was the fans. sCO_2

flow rate can be adjusted to demonstrate achieving full design temperatures at the maximum available heat input.

Pressure Drop and Flow Distribution

Pressure drops in the model were limited to the heated tubes, while the test data includes header entrance and exit losses, as well as external piping, and flow balancing valves. The model predicted a total pressure drop of 0.36 MPa while the test data indicates of the pressure drop to be 0.47 MPa. This leaves a difference of 0.11 MPa that is unaccounted for in the model. A few obvious factors were investigated to account for this discrepancy.

At the time the baseline model was developed, external piping had not been designed. Test data shows losses on the order of 0.03MPa. Additionally, the effects of the balancing valves are not entirely known because the valve positions were not recorded in the dataset. Procedural changes have since been implemented, ensuring that the valve positions are recorded to improve accuracy of this calculation.

From fully open to 50% open, the valves are designed to contribute between 0.02 and 0.05 MPa. However, if the valves were closed to the maximum acceptable level of 20% open, they would contribute 0.45 MPa to the total dP. Without documented valve positions, we assumed a position of 75% open, adding a pressure loss of 0.03 MPa. Incorporating the external piping and valve losses results in a predicted total pressure drop of 0.42 MPa, equivalent to 89% of the measured values. These calculations were considered acceptable, enabling reliable predictions during future modeling efforts without significant revisions.

Generally, a surface can be expected to have temperature maldistribution proportional to the overall temperature rise between inlet and outlet. Considering the overall temperature change in the radiant panels of 178°C, a normal temperature distribution would be +/- 50°C. The data in Table 8 matches the prediction well, with the distribution in the convective section ~15°C, while the radiant tubes show a worst case of ~45 °C which can be tightened considerably using the balancing valves as shown in the “adjusted” column.

Table 8: Tube to Tube Temperature Distribution.

	CO_2 Temps at Convective Outlet °C	CO_2 Temps at Radiant Outlet (unbalanced) °C	CO_2 Temps at Radiant Outlet (adjusted) °C
1	371	552	563
2	370	544	556
3	366	553	565
4	368	547	556
5	367	557	567
6	364	550	555
7	354	551	564
8		556	554
9		61*	59*
10		548	555
11		554	561
12		560	567
13		562	584
14		583	564
15		563	583
16		590	583

**The values indicated in red are from unreliable instruments*

Conclusions

Conclusions from CFD-Guided Design of the Primary Heat Exchanger

1. The L1500 will need to operate at a firing rate near 6 MMBtu/hr in order to achieve the design heat transfer to the PHX feeding the Thermal Management System with a load of 1.26 MW.
2. Care will have to be taken in the installation and operation of the PHX to keep the peak heat flux at or below 175,000 W/m2.
3. Moving the crossmembers of the PHX closer to the burner and extending the heat transfer surface is expected to reduce the peak heat flux achieve a heat flux near the target at a firing rate of 6 MMBtu/hr.
4. Increasing the excess air will also reduce the peak heat flux, by reducing the adiabatic flame temperature.
5. All efforts to extend the heat release profile by extending the flame (staging, reduced swirl and increased primary velocity) are expected to increase the peak heat flux to the PHX by either increasing the mixing downstream in the furnace or reducing the local stoichiometry which in turn increases the adiabatic flame temperature.

Conclusions from Primary Heat Exchanger Design

1. The PHX performed well in all testing to date. Temperature readings on the flux sensors indicated that the unit was operating at safe conditions considering the reduced operating pressures. The tube mid wall temperatures need to be monitored if operating pressure is increased, as they may have exceeded the recommended values for those conditions. Ideally, the unit would get more test time to determine any medium-term impacts of sCO_2 on the tube metals. No signs of overheating or damage have been noted so far.
2. Based on the data available to date, the unit is behaving close to expectations for total absorption, with the unit slightly outperforming the baseline model. Additional work will be done on the model to enhance its fit to the data and carry that level of accuracy into larger scale designs.
3. Pressure drops through the system align with predictions sufficiently, providing a good level of confidence moving forward. Flow distribution within the radiant portion of the PHX was reasonable with all valves fully open and improved by adjusting the valves. More testing is required to determine the impact of flow distribution on final temperatures. A target pressure drop for large scale applications to maintain flow balance can be determined once this additional testing is complete.
4. Flux sensor readings require additional review and more data collection to verify. Initial values showed a relatively flat flux profile as compared to both the transient and CFD modeling. It is possible that the coal burn out time in these models was not accurate resulting in a different flux distribution. Alternatively, there may be an issue with the readings from the flux sensors, or the correlation used to calculate flux from the individual temperature measurements. Additional testing with longer durations will determine if this is related to refractory temperatures, fuel mixing, or other effects.
5. This testing has allowed us to reduce risk profiles for major aspects of the design, including the manufacturing process for stainless steel membrane panels, and the overall heat transfer calculations. These areas were significant barriers to deploying this technology at a larger scale with appropriate costs, and this reduction in risk will improve design margins accordingly. Larger-scale deployments will further improve all areas of the design and manufacturing process.

References

[1] F. Crespi, G. Gavagnin, D. Sánchez, G.S. Martínez, Supercritical carbon dioxide cycles for power generation: A review, Applied Energy, 195 (2017) 152-183.

[2] Y. Liu, Y. Wang, D. Huang, Supercritical CO2 Brayton cycle: A state-of-the-art review, Energy, 189 (2019) 115900.

[3] J. Syblik, L. Vesely, S. Entler, J. Stepanek, V. Dostal, Analysis of supercritical CO2 Brayton power cycles in nuclear and fusion energy, Fusion Engineering and Design, 146 (2019) 1520-1523.

[4] P. Wu, Y. Ma, C. Gao, W. Liu, J. Shan, Y. Huang, J. Wang, D. Zhang, X. Ran, A review of research and development of supercritical carbon dioxide Brayton cycle technology in nuclear engineering applications, Nuclear Engineering and Design, 368 (2020) 110767.

[5] M. Mecheri, Y. Le Moullec, Supercritical CO2 Brayton cycles for coal-fired power plants, Energy, 103 (2016) 758-771.

[6] E. Ruiz-Casanova, C. Rubio-Maya, J.J. Pacheco-Ibarra, V.M. Ambriz-Díaz, C.E. Romero, X. Wang, Thermodynamic analysis and optimization of supercritical carbon dioxide Brayton cycles for use with low-grade geothermal heat sources, Energy Conversion and Management, 216 (2020) 112978.

[7] P. Garg, P. Kumar, K. Srinivasan, Supercritical carbon dioxide Brayton cycle for concentrated solar power, The Journal of Supercritical Fluids, 76 (2013) 54-60.

[8] G. Manente, F.M. Fortuna, Supercritical CO2 power cycles for waste heat recovery: A systematic comparison between traditional and novel layouts with dual expansion, Energy Conversion and Management, 197 (2019) 111777.

[9] L. Sun, D. Wang, Y. Xie, Thermodynamic and exergoeconomic analysis of combined supercritical CO2 cycle and organic Rankine cycle using CO2-based binary mixtures for gas turbine waste heat recovery, Energy Conversion and Management, 243 (2021) 114400.

[10] O.H. Díaz-Ibarra, J. Spinti, A. Fry, B. Isaac, J.N. Thornock, M. Hradisky, S. Smith, P.J. Smith, A Validation/Uncertainty Quantification Analysis for a 1.5 MW Oxy-Coal Fired Furnace: Sensitivity Analysis, Journal of Verification, Validation and Uncertainty Quantification, 3 (2018).

[11] T. Allgurén, K. Andersson, A. Fry, E.G. Eddings, NO formation during co-combustion of coal with two thermally treated biomasses, Fuel Processing Technology, 235 (2022) 107365.

[12] S. Fakourian, X. Li, Y. Wang, J.O.L. Wendt, A. Fry, Ash Aerosol and Deposit Formation from Combustion of Coal and Its Blend with Woody Biomass at Two Combustion Scales: Part 1─1.5 MWTH Pilot-Scale Combustor Tests, Energy & Fuels, 36 (2022) 554-564.

[13] R. Roy, B. Schooff, X. Li, S. Montgomery, J. Tuttle, J.O.L. Wendt, K. Dickson, B. Iverson, A. Fry, Ash aerosol particle size distribution, composition, and deposition behavior while co-firing coal and steam-exploded biomass in a 1.5 MWth combustor, Fuel Processing Technology, 243 (2023) 107674.

[14] R. Roy, S. Bandi, X. Li, B. Schooff, R. Kuttler, M. Aichele, S. Montgomery, J. Tuttle, S.J. Smith, J.O.L. Wendt, B.D. Iverson, A. Fry, Synergistic reduction of SO2 emissions while co-firing biomass with coal in pilot-scale (1.5 MWth) and full-scale (471 MWe) combustors, Fuel, 358 (2024) 130191.

[15] A. Maxson, J. Miller, D. Buckmaster, T. Thome, B. Sakadjian, R. Chamberland, K. Hong, & D. Hogg. High-Efficiency Thermal Integration of Closed Supercritical CO2 Brayton Power Cycles with Oxy-Fired Heaters (Final Report). United States.

Acknowledgement

The authors express their sincere gratitude to Scott Montgomery of the San Rafael Energy Research Center for his unwavering commitment to the project. Scott and his team played a crucial role in the program's success, and their dedication is greatly appreciated.

Disclaimer

This material is based upon work supported by the Department of Energy under Award Number DE-FE0031928. This report was prepared as an account of work sponsored by an agency of the United States Government. Neither the United States Government nor any agency thereof, nor any of their employees, makes any warranty, express or implied, or assumes any legal liability or responsibility for the accuracy, completeness, or usefulness of any information, apparatus, product, or process disclosed, or represents that its use would not infringe privately owned rights. Reference herein to any specific commercial product, process, or service by trade name, trademark, manufacturer, or otherwise does not necessarily constitute or imply its endorsement, recommendation, or favoring by the United States Government or any agency thereof. The views and opinions of authors expressed herein do not necessarily state or reflect those of the United States Government or any agency thereof.

CRediT Authorship Statement

Kyle P. Sedlacko: Investigation, Formal analysis, Writing - Review & Editing. **Jason Miller:** Project administration, Funding acquisition, supervision. **Brett Bowan:** Investigation, Writing. **Timothy Held:** Conceptualization, Funding acquisition, Project administration **Andrew Fry:** Conceptualization, Resources, Supervision, Funding acquisition, Investigation. **Brian Schooff:** Investigation, Formal analysis, Writing - Review & Editing. **Rajarshi Roy**: Investigation, Formal analysis, Writing - Review & Editing. **Michael D. Johnson:** Methodology, Formal analysis, Investigation, Writing. **Andrew P. Chiodo:** Investigation, Software, Validation, Formal analysis, Writing – Review & Editing, Visualization